

DESY SR-86-05  
June 1986

X-RAY STANDING WAVE STUDIES OF GERMANIUM ADSORBED  
ON Si(111) SURFACES

by

Eigentum der Property of	<b>DESY</b>	Bibliothek library
Zugang: Accessions:	01. SEP. 1986	
Leihfrist: Loan period:	7	Tage days

B.N. Dev, G. Materlik

*Hamburger Synchrotronstrahlungslabor HASYLAB at DESY*

R.L. Johnson

*Max-Planck-Institut für Festkörperforschung, Stuttgart*

W. Kranz, P. Funke

*II. Inst. für Experimentalphysik, Universität Hamburg*

ISSN 0723-7979

DESY behält sich alle Rechte für den Fall der Schutzrechtserteilung und für die wirtschaftliche Verwertung der in diesem Bericht enthaltenen Informationen vor.

DESY reserves all rights for commercial use of information included in this report, especially in case of filing application for or grant of patents.

To be sure that your preprints are promptly included in the  
HIGH ENERGY PHYSICS INDEX,  
send them to the following address ( if possible by air mail ) :

DESY  
Bibliothek  
Notkestrasse 85  
2 Hamburg 52  
Germany

X-Ray Standing Wave Studies of Germanium Adsorbed on Si(111) Surfaces

B.N. Dev and G. Materlik

Hamburger Synchrotronstrahlungslabor HASYLAB at DESY,  
Notkestr. 85, D-2000 Hamburg 52, FRG

R.L. Johnson

MPI für Festkörperforschung, Heisenbergstr. 1,  
D-7000 Stuttgart 80, FRG

W. Kranz and P. Funke

II. Inst. für Experimentalphysik, Universität Hamburg,  
Luruper Chaussee 149, D-2000 Hamburg 50, FRG

Abstract

The positions of germanium atoms adsorbed on Si(111) surfaces have been determined with x-ray standing waves. Ge atoms have been found to occupy the atop site and/or vacancies in the inner layer of the substrate surface bilayer for the (1x1) superstructure. For the (7x7) structure, our results support the dimer adatom stacking-fault model of Takayanagi et al. for the bare silicon surface. Ge atoms occupy the surface-atop and the adatom-atop sites on this structure. A higher binding energy for the surface-atop site is indicated from the growth of germanium at different substrate temperatures.

to be published in: Surf. Scie.

1. Introduction

The geometrical structures of surfaces and the way they change upon addition of a second material affect the electronic properties across the interface. Several techniques for surface and interface structural determination, using x-rays, e.g. surface extended x-ray absorption fine structure (SEXAFS), kinematical total reflection Bragg diffraction (TRBD), x-ray standing waves (XSW), have been developed over the recent years. In the present work X-ray standing waves were applied to determine the location of germanium atoms adsorbed on silicon (111) 1x1 and 7x7 surfaces. Another motivation was to understand the structure of the host surfaces through the structure of the Ge-adsorbed surfaces and the chemical similarity (isoelectronic valence shell) of germanium and silicon.

The formation and characteristics of x-ray standing waves can be described in a simplified way as follows. When a plane wave x-ray beam is Bragg diffracted by a perfect crystal, a standing wave field is generated inside the crystal due to the interaction of the coherently related incident and diffracted plane waves [1]. Two important characteristics of the standing wave field are that the antinodal (or nodal) planes are parallel to and have the same periodicity as the diffraction planes. The phase relationship between the incident and the diffracted electric field amplitudes  $E_0$  and  $E_H$ , respectively, determines the position of the antinodal planes relative to the diffraction planes. Within a narrow angular region close to the Bragg angle ( $\theta_B$ ), the complex quantity  $E_H/E_0$  continuously changes phase, resulting in a continuous movement of the antinodal planes through half the planar distance. Thus, by varying the angle of incidence ( $\theta$ ), it is possible to modulate the E-field intensity to which an atom at a particular location inside the crystal is exposed. The angular response of a secondary process, such as

fluorescence, which is proportional to the x-ray intensity at the center of the atom, depends thus on the position of the atom [2]. The fact that the standing wave field, with unaltered characteristics, extends outside the crystal surface into the vacuum or a thin epitaxial layer allows the positional determination of adsorbed atoms on crystal surfaces [3,4] or atoms at the interface [5,6]. The combination of XSW with highly intense synchrotron radiation opens up a wide field of applications [7].

## 2. Experimental

Silicon (111) samples of  $1 \times 1 \text{ cm}^2$  area and 0.1-0.2 cm thickness were sputter cleaned with argon ion bombardment and annealed at  $\sim 950^\circ\text{C}$  in an ultra high vacuum (UHV) chamber at a base pressure of  $10^{-10}$  torr. Following the annealing, a slow cooling of the sample gave rise to a low energy electron diffraction (LEED) pattern of  $7 \times 7$  superstructure, whereas the  $1 \times 1$  structure was obtained by rapid cooling. Surface cleanliness was checked with ultraviolet photoemission spectroscopy (UPS) by monitoring the silicon valence band (VB) spectrum prior to germanium evaporation. Upon germanium deposition, for a coverage range of 0.1-1.0 monolayer (ML), the respective LEED patterns remained unchanged. Cleanliness was again checked by monitoring the germanium 3d line shape and intensity, in addition to the silicon VB, in the photoemission spectra. For most of the preparations, the substrate was maintained at room temperature during Ge evaporation, and annealed at  $450^\circ\text{C}$  afterwards. However, Ge was also evaporated directly onto a hot ( $530^\circ\text{C}$ ) substrate.

The samples were prepared in the preparation chamber at the FLIPPER II station at HASYLAB and transferred in a small UHV "baby" chamber to the wiggler station for XSW measurements. During the transfer and the measurements the vacuum maintained was  $10^{-9}$  torr or better.

The x-ray standing wave experimental set-up is schematically shown in Fig. 1. White x-radiation emerging from a 32-pole wiggler enters the evacuated monochromator chamber. The monochromatic beam continues to be in high vacuum until it enters the experimental hutch. This arrangement, reducing the absorption of low energy photons in air, offers the possibility of using photons of energy down to approximately 3 keV. The higher intensity of the wiggler beam ( $\sim 10$  times compared to a DURIS bending magnet at  $\sim 10$  keV photon energy and 3.7 GeV electron energy) allows measurements on small sample areas, which may be a necessity because of the partial loss of quality of the sample crystal during preparation. The heat load on the first monochromator crystal due to the high intensity of the wiggler beam makes it necessary to cool the crystal. The monochromator crystals are chosen to suit a particular experiment. For example, for the XSW measurements with silicon (111) reflection, Si(111) crystals are used for monochromatization in order to make the set-up nondispersive. Though for an XSW measurement one needs, in principle, an incident plane wave ( $e^{i\mathbf{k}\cdot\mathbf{r}}$  with constant  $\mathbf{k}$ ), one can prepare, with an usable intensity, only a beam with a narrow range of  $\Delta\mathbf{k}$ . The monochromatization reduces the range of  $|\mathbf{k}|$ . The reduction in the angular divergence of  $\mathbf{k}/|\mathbf{k}|$  is obtained by the defocussing symmetric-asymmetric combination of the monochromator crystals. Thus the exit beam from the monochromator, being compressed both in energy and angular range, is very close to a plane wave.

The UHV sample chamber, used also in IRBD experiments [8], is small, light and transportable. Therefore, it can be mounted easily on a two-stage ( $\theta, \phi$ ) goniometer. When the sample is placed at a Bragg angle, the Bragg-diffracted photons are detected in the NaI(Tl) detector while the Si(Li) detector (looking perpendicular to the plane of the figure) is used to detect the photons originating from inelastic processes. The ionization chambers monitor the incident intensity in front of and behind the slit system. The signal from

the ionization chamber before the slit system is used in a feedback loop for stabilizing the monochromator output. In the present series of experiments, the  $K_{\alpha}$  fluorescence photons from the adsorbed germanium atoms were detected in the Si(Li), simultaneously with the reflected beam in the NaI(Tl), while the energy  $E_{\gamma}$  of the beam incident on the sample was varied by rocking in a parallel mode the first and the second crystal of the monochromator [9]. (Varying  $E_{\gamma}$  of the incident beam and varying the angle of incidence by turning the sample are in the present case equivalent, because either method can sweep through the Bragg reflection of the sample crystal.

The quality of the crystal is crucial for XSW measurements. In order to ensure a sufficient quality, double crystal topography [10] was performed on the samples. In fact, strain patterns introduced by sputtering and annealing were observed across the surface of the crystal. A perfect region down to an area of  $\sim 0.2 \text{ mm}^2$  was selected with a slit system for the measurements.

### 3. Results and Discussion

For an incident  $\sigma$ -polarized plane wave x-ray beam which is Bragg diffracted [11] from a symmetrically cut crystal, the fluorescence yield from the adsorbed atoms for a given reflection ( $H$ ) is:

$$A(\vartheta) = A_0 [1 + R(\vartheta) + 2\sqrt{R(\vartheta)} f_c \cos[\nu(\vartheta) - 2\pi\phi]] \quad (1)$$

where  $R(\vartheta)$  is the reflectivity,  $\nu(\vartheta)$  is the phase of the diffracted E-field amplitude relative to the incident one. The quantities  $\phi$  and  $f_c$  are called coherent position and coherent fraction, respectively, and are closely related to the actual position of the adsorbed atoms and the fraction of the total number of atoms at this position.  $A_0$  is the yield at zero reflectivity of

the  $(hkl)$  reflection. The quantities  $\phi$  and  $f_c$  are obtained by a least-squares fit of the normalized fluorescence yield,  $Y(\vartheta) = A(\vartheta)/A_0$ , to Eqn. (1).

#### 3.1 Germanium on Silicon (111) 1x1

Fig. 2 shows the results of a measurement on a Si(111) 1x1-Ge sample with (111) reflection. The coherent position,  $\phi$ , was found to be the same within the experimental error for as-grown and for annealed (2 min at 450°C) samples. However, the coherent fraction,  $f_c$ , increased slightly after annealing. The observed coherent position can be explained by the adsorption of Ge at the atop site and/or at an available vacancy in the second layer of the substrate. The corresponding model is shown in the inset of Fig. 2. From the chemical similarity of germanium and silicon it is easy to conceive a germanium atom at the substitutional site covalently bonded with four Si atoms in a tetrahedral configuration. However, at the atop site, Ge contributing four electrons and Si one, the picture of bonding is not clear. In fact, one may wonder whether the binding at the atop site is at all possible. A molecular calculation involving one H atom and one Si atom, which offers a similar situation, however, suggests the possibility of binding [12].

In the present analysis a Si-Ge bond length of 2.40 Å, which is the average of Si-Si bond length in silicon crystal and the Ge-Ge bond length in germanium crystal, has been assumed. The Ge atom at the atop site is at a distance of  $(2.40+0.39)\text{Å}$  or  $0.89 d_{111}$  ( $d_{111} = 3.14 \text{ Å}$  for silicon) from the surface diffraction plane. The Ge atom at the substitutional site is also at a distance of  $0.89 d_{111}$  from the second diffraction plane (or at  $-0.11 d_{111}$  from the surface diffraction plane). Therefore, the joint response of the atoms from these two sites gives rise to a coherent position of  $0.89 d_{111}$ . For atoms at different distances from the diffraction planes the coherent position depends on the relative population at these distances [13].

Measurements made on different spots of the same sample as well as on samples from different preparations, showed variations in  $f_c$  but not in  $\phi$ .

This supports the assumption of a one position model. The large incoherent fractions observed in the present study are also consistent with the high degree of disorder observed by channeling for the Si(111)-Ge system [14].

### 3.2 Germanium on Si(111) 7x7

The results of one measurement using a silicon (111) reflection, and one with a (220) reflection are shown in Figs. 3 and 4, respectively. The proposed model for Si(111) 7x7-Ge is shown in Fig. 5. The model shows the Ge atoms at the surface-atop (A, B in Fig. 5) and adatom-atop (C, D, E, F in Fig. 5) sites on the dimer adatom stacking-fault (DAS) model of bare Si(111) 7x7 surface proposed by Takayanagi et al. [15]. If only the surface atop site is occupied, the coherent position would be, like the 1x1 case,  $0.89 d_{111}$ . When only the adatom-atop site is occupied, the coherent position would be  $1.14 d_{111}$ . Occupation of both these sites with equal population would give rise to a coherent position of  $1.02 d_{111}$ . The measured coherent positions of  $1.06 \pm 0.02$  (Fig. 3) and  $0.98 \pm 0.02$  (not shown in the figure) for germanium coverages of 0.5 ML and 0.08 ML, respectively, can be explained by assuming that at lower coverage more surface-atop sites (position 0.89) are occupied, and with increasing coverage, the surface-atop sites having been filled, the only available adatom-atop (position 1.14) sites are occupied. (There are 12 adatom-atop sites and 6 surface-atop sites per 7x7 unit cell.) This assumption is corroborated by the results of (220) reflection measurements, which are shown in Fig. 4 for a germanium coverage of 0.2 ML deposited on a hot (530°C) substrate. The observed coherent position of  $(0.85 \pm 0.02) d_{220}$  can be explained in terms of the occupation of the surface-

atop sites only (A, B). Because of the presence of stacking-faults on one half, the projections of A and B atoms along the <220> direction are  $d_A = 1.02 d_{220}$  and  $d_B = 0.69 d_{220}$ , respectively. The respective fluorescence response curve would be those shown by curve a and b in Fig. 4. The joint response is shown by the fitted curve. Occupation of the sites C, D etc. would give rise to a joint response very similar to the curve b (because  $d_B = d_C = d_D$ ). The proposed model is consistent with both (111) and (220) reflection measurements. The occupation of only surface-atop-site on hot substrate is an indication of higher binding energy for germanium at the surface-atop site compared to the adatom-atop site.

Our measured coherent positions for (111) reflection do not differ much from those of Patel et al. [16]. However, their (220) results differ significantly from ours. Their XSW measurements were not made under UHV environment, but on UHV prepared interfaces covered with amorphous silicon.

### 4. Conclusions

In the present work we have investigated the structures of Si(111)-Ge system for (1x1) and (7x7) superstructures. For (1x1) case Ge atoms appear to occupy the atop site and/or the vacancy in the inner layer of the surface silicon double layer. By measuring the distance components in the <111> and <220> directions the positions of the Ge atoms on a Si(111) 7x7 surface have been determined. The results support the dimer adatom stacking-fault model of Takayanagi et al. [15] for the bare Si(111) 7x7 surface. Ge atoms are at the surface-atop and the adatom-atop sites. Measurements on samples grown at different substrate temperatures have led to the conclusion that the binding energy for the surface-atop site is higher compared to the adatom-atop site.

Acknowledgement

The financial support of this project by the Bundesminister für Forschung und Technologie is gratefully acknowledged.

References

1. M. von Laue, Röntgenstrahlinterferenzen (Akademische Verlagsgesellschaft, Frankfurt, 1960)
2. B.W. Batterman, Phys. Rev. A153 (1964) 759
3. P.L. Cowan, J.A. Golovchenko and M.F. Robbins, Phys. Rev. Lett. 44 (1980) 1680
4. G. Materlik, A. Frahm and M.J. Bedzyk, Phys. Rev. Lett. 52 (1984) 441
5. K. Akimoto, I. Ishikawa, T. Takahasi and S. Kikuta, Jap. J. Appl. Phys. 22 (1983) L789
6. E. Vlieg, A.E.M.J. Fischer, J.F. van der Veen, B.N. Dev and G. Materlik, Abstracts of the 8th European Conference on Surface Science, p. 93, Surf. Sci.(to be published)
7. G. Materlik, Z. Phys. B61 (1985) 405
8. J. Bohr, R. Feidenhans'l, M. Nielsen, M. Toney, R.L. Johnson and I.K. Robinson, Phys. Rev. Lett. 54 (1985) 1275
9. P. Funke and G. Materlik, Solid State Comm. 54 (1985) 921
10. U. Bonse and C. Kappler, Z. Naturforschung 13a (1958) 792
11. Bragg's law:  $k_{\parallel} - k_{\perp} = H$  ;  $k_{\perp}$  and  $k_{\parallel}$  are incident and diffracted wave vectors, respectively.  $H$  ( $|H| = 1/d_{hkl}$ ) is a reciprocal lattice vector.
12. K.Hermann and P.S. Bagus, Phys. Rev. 20 (1979) 1603
13. B.N. Dev, V. Aristov, N. Hertel, T. Thundat and W.M. Gibson, Surf. Sci. 163 (1985) 457
14. H.J. Gossmann, L.C. Feldmann and W.M. Gibson, Surf. Sci. 155 (1985) 413
15. K. Takayanagi, Y. Tanishiro, M. Takahashi and S. Takahashi, J. Vac. Sci. Technol. A3 (1985) 1502
16. J.R. Patel, J.A. Golovchenko, J.C. Bean and R.J. Morris, Phys. Rev. 31 (1985) 6884

Figure Captions

Fig. 1 Schematic layout of the set-up for x-ray standing wave experiments at the wiggler beamline at HASYLAB.

Fig. 2 Ge on Si(111) 1x1. Experimental data points and the theoretical curves for the normalized Ge  $K_{\alpha}$  fluorescence yield,  $Y(\theta)$ , and silicon (111) reflectivity,  $R(\theta)$ , as a function of reflection angle. The inset shows the model of the Si(111) 1x1-Ge interface with the Ge atoms at the atop site and at a vacancy in the inner layer of the surface silicon double-layer.

Fig. 3 Ge on Si(111) 7x7. Ge  $K_{\alpha}$  fluorescence yield,  $Y(\theta)$ , and reflectivity,  $R(\theta)$ , for a measurement with a silicon (111) reflection.

Fig. 4 Ge on Si(111) 7x7. Ge  $K_{\alpha}$  fluorescence yield,  $Y(\theta)$ , and reflectivity,  $R(\theta)$ , for a measurement with a silicon (220) reflection. Curves a and b are those expected from the atom at A and at B (Fig. 5), respectively. The effective response due to occupation of both A and B sites is given by the fitted curve,  $Y(\theta)$ .

Fig. 5 Model of Si(111) 7x7-Ge interface showing the Ge atoms at the surface-atop (A, B) and the adatom-atop (C, D, E, F) sites on the dimer adatom stacking-fault model of Si(111) 7x7 surface. Region I shows a part of the unit cell that has normal stacking (123456), and II shows the stacking-fault (56').

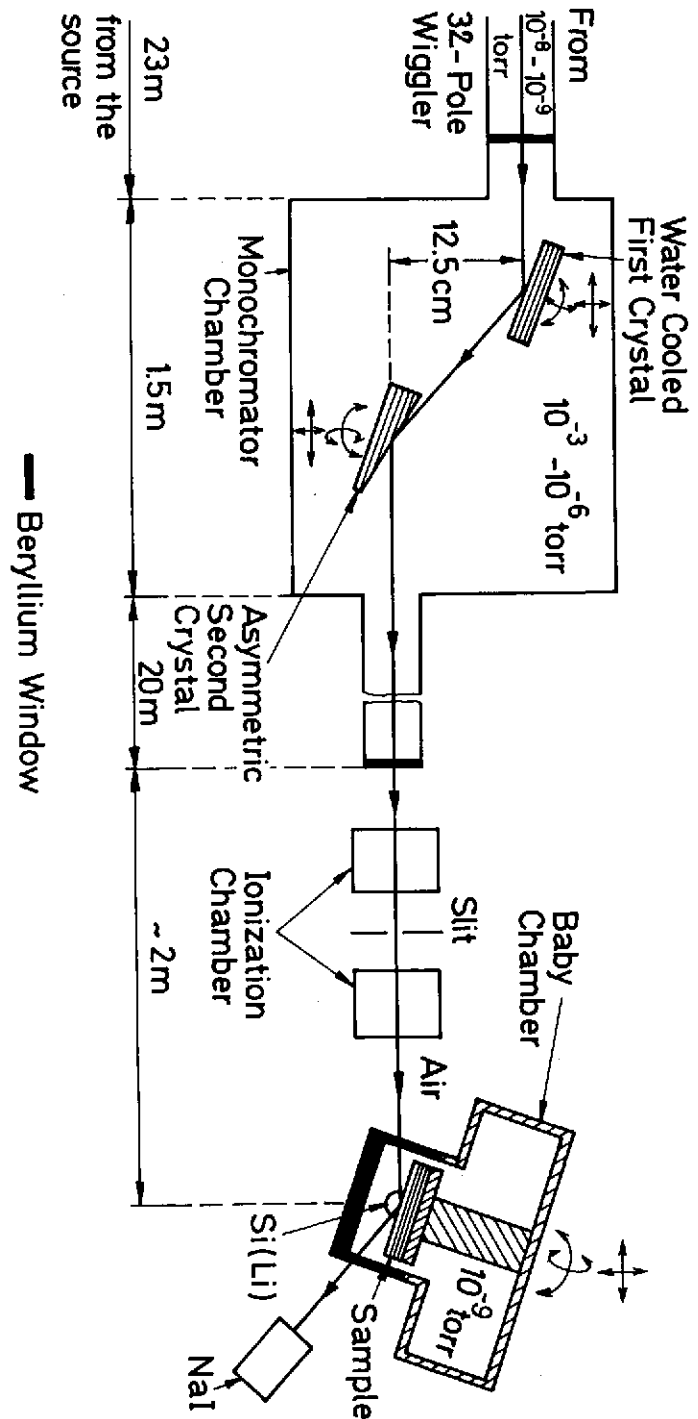


Fig. 1



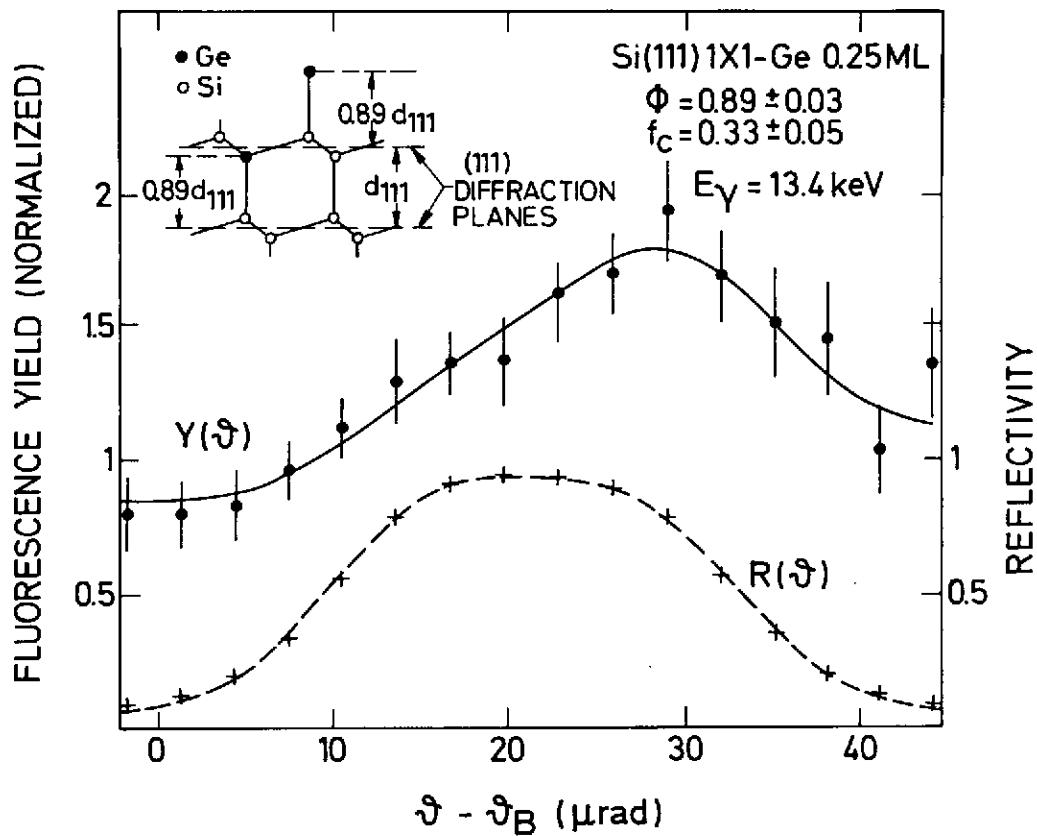


Fig. 2

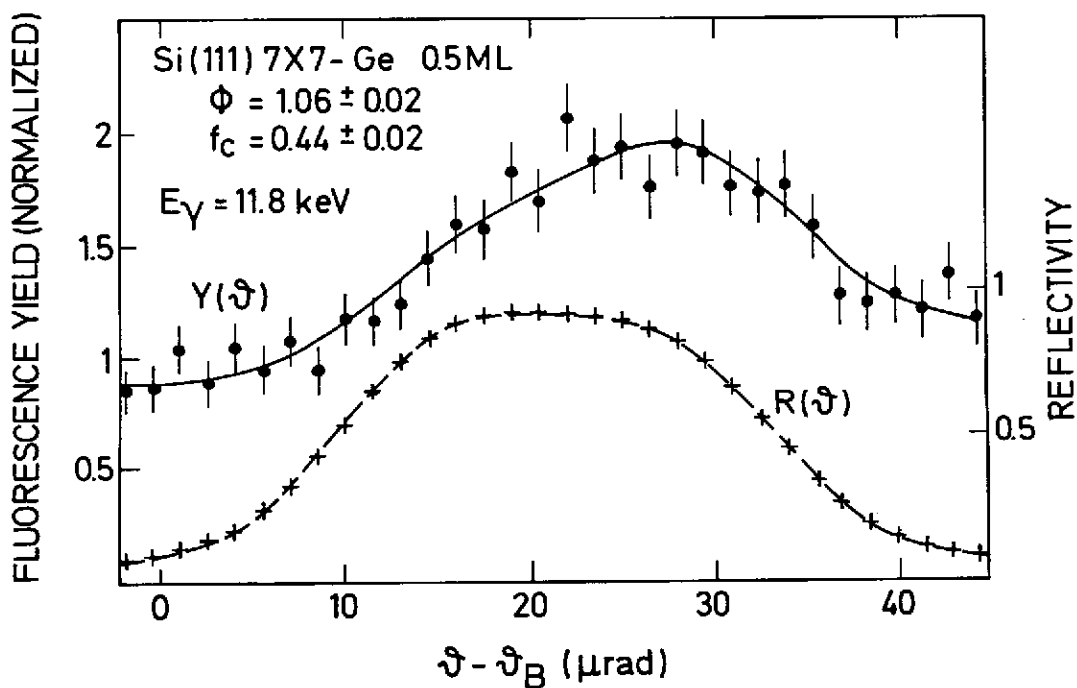


Fig. 3

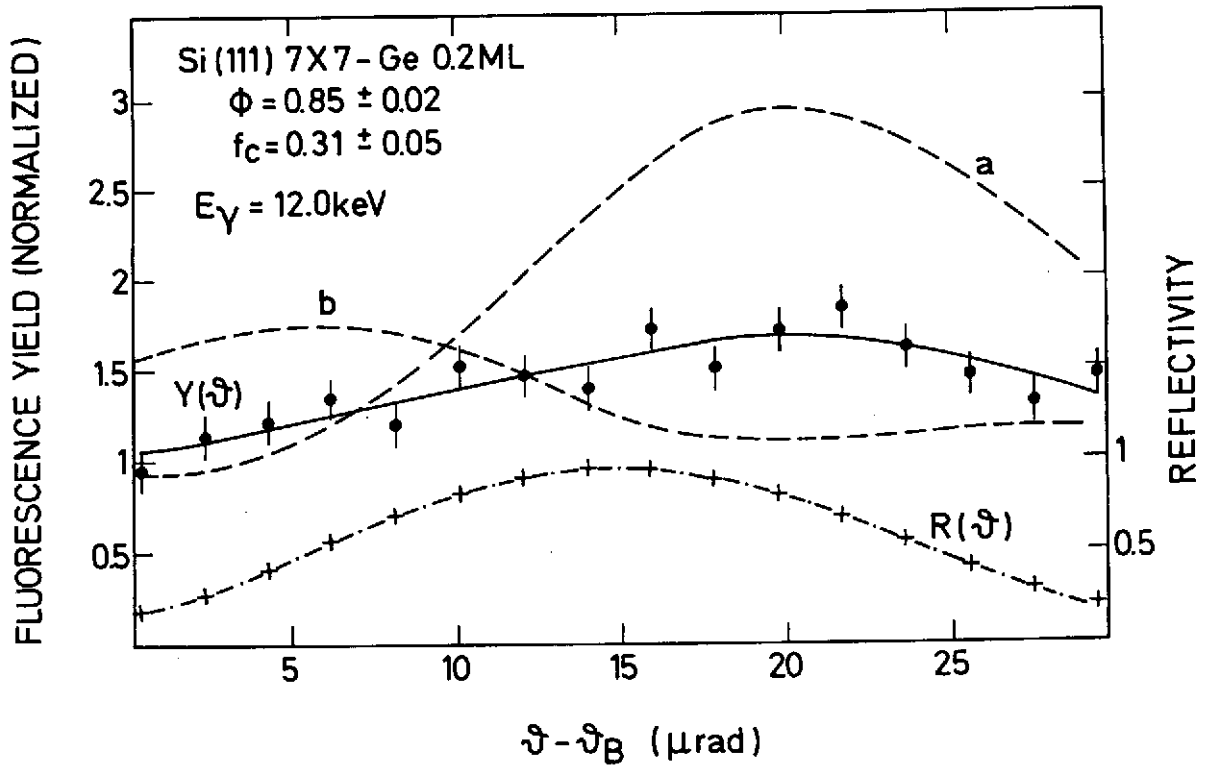


Fig. 4

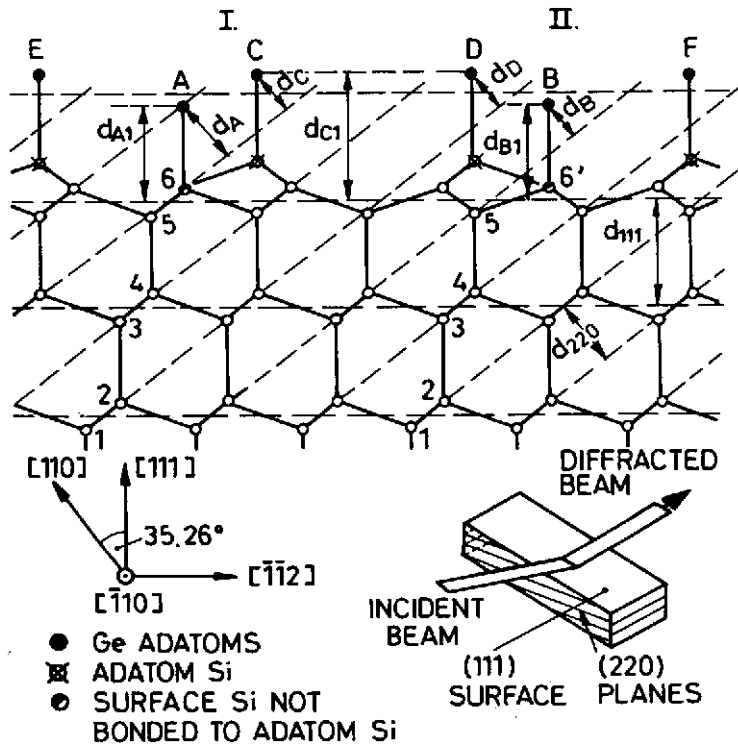


Fig. 5